Excitation spectrum of multiferroics at finite temperatures

Thomas Michael* and Steffen Trimper†
Institute of Physics, Martin Luther University, D-06099 Halle, Germany
(Received 13 August 2010; revised manuscript received 18 November 2010; published 11 April 2011)

A systematic microscopic theory of the magnetoelectric (ME) effect in multiferroic materials with well-separated phase-transition temperatures is presented. Whereas the ferroelectric subsystem is described by an Ising model in a transverse field, the magnetic one is characterized by the Heisenberg model with Dzyaloshinski-Moriya interaction (DMI). The symmetry-allowed quartic coupling between both subsystems, and the application of a Green's function technique in a dynamical mean-field approximation, exhibit the calculation of the elementary excitations analytically, which are mutually influenced by the respective other subsystem. The magnetic excitation is a Goldstone mode, while the ferroelectric dispersion relation shows a soft-mode-like behavior. We find the macroscopic polarization and the transverse magnetization in a broad temperature interval up to the corresponding phase-transition temperatures (type-I multiferroics). Due to the DMI, the system offers different spiral structures, which are incorporated into the model by using a transformation of the underlying spin operators into a representation without a fixed quantization axis. The polarization increases at the magnetic phase-transition temperature, and is also enhanced by increasing the ME coupling strength as well as the DMI. We demonstrate likewise the variation of the spin-wave dispersion relation with the ME coupling strength and the DMI. As a consequence, the macroscopic magnetization is enhanced with increasing coupling.

DOI: 10.1103/PhysRevB.83.134409 PACS number(s): 75.10.Jm, 77.55.Nv, 75.30.Ds, 75.25.−j

I. INTRODUCTION

The study of the broad diversity of spin arrangements is strongly advanced by the search for new types of order in magnetoelectric multiferroics, where magnetic and ferroelectric order can coexist.[1–3] Due to symmetry-allowed magnetoelectric (ME) couplings, such multiferroics exhibit control of magnetic properties by electric fields and, vice versa, ferroelectric order by magnetic fields. According to Refs. 3 and 4, one has to distinguish between two kinds of multiferroics. Type-I multiferroics are characterized by well-separated phase-transition temperatures of the underlying ferroelectric and magnetic subsystem. The temperature scale for the ferroelectric order is much larger than for the magnetic one. Representative examples offering such a behavior are the transition-metal perovskites $BiFeO_3$, where ferroelectricity is caused by the ordering of lone pairs of two outer electrons and the hexagonal $R MnO_3$ compound.[1,5,6] In other type-I compounds, such as $Pr_1/2Ca_1/2MnO_3$ (see Ref. 7), the ferroelectric properties are due to charge ordering. Such an ordering mechanism is characteristic for the occurrence of a polarization. Furthermore, it seems reasonable that the coupling between the ferroelectric and the magnetic subsystem are assumed to be weak. In the second class, the type-II multiferroics, the ferroelectric order is directly accompanied by a magnetic order. A feature of this magnetic multiferroics is the occurrence of an electric polarization due to a spiral magnetic ordering.[5,8,9] Here the coupling is assumed to be strong. Such noncollinear structures can be described on a microscopic[10,11] and a mesoscopic level.[12] The realization of various types of multiferroics depends in a significant manner on the symmetry. Thus, transition metals $R MnO_3$ with an orthorhombic structure are of type II, with narrow phase-transition temperatures. A common explanation of spiral alignment due to a competition between nearest and next-nearest neighbors does not reflect the breaking of inversion symmetry, which is characteristic for a ferroelectric system. Otherwise, it is well known that the relativistic Dzyaloshinski-Moriya interaction (DMI) plays an important role in systems without inversion symmetry.[13,14] The relationship between ferroelectricity and DMI is discussed in Ref. 15, multiferroic perovskites are analyzed in Ref. 16, and an exchange bias driven by DMI in antiferromagnetic interfaces is discussed in Ref. 17. Recently the dynamical interplay between ferroelectricity and magnetism has been analyzed under the inclusion of the DMI.[18]

In view of broad applications of different ME devices, giving rise to the coupling between magnetism and ferroelectricity, the general mechanism should be elucidated. Despite the great progress in the experimental characterization of ME material, the discussion of the properties in terms of microscopical models is quite rare. One of the most prominent approaches seems to be first-principles studies, which are based on the density functional theory.[19,20] In Ref. 21, the ME effect has been investigated theoretically in ferroelectromagnets under the aspects of the origin of the ME effect, identified with the dielectric changes and the ME response. The magnetocapacitance effects in $BiMnO_3$ have been interpreted in Ref. 22, applying a Ginsburg-Landau theory in terms of the two order parameters P and M for the polarization and the magnetization, respectively. The model includes a coupling term proportional to P^2M^2 in the thermodynamic potential and offers a second-order phase transition of the ferroelectromagnets.

Otherwise the properties of solid materials are characterized by their elementary excitations. In this paper we emphasize that multiferroics also offer such a spectrum of elementary excitations, which determines the macroscopic behavior of the system as magnetization and polarization. To that aim, we start from a microscopic model comprised of a ferroelectric and a magnetic subsystem, as well as a symmetry-allowed coupling between both. The magnetic part is described by the isotropic Heisenberg model expressed by spin operators

and an additional DMI, which gives rise to a spiral magnetic order. The ferroelectric subsystem is characterized by charge-ordering processes, which can be mapped onto an Ising model in a transverse field in terms of pseudospin variables.[23] The coupling between the subsystems is assumed to be biquadratic in both sets of variables, as already proposed in Ref. 22. Such a coupling is realized, for instance, in the hexagonal version of $RMnO_3$, and was previously studied in Refs. 24–26, but without the consideration of spiral structures. Because this material is of type I, the interaction between both systems is assumed to be weak and, hence, the model is treated in a kind of dynamical mean-field approximation. The coupled system is studied by a thermodynamic Green's function technique, which allows immediately the determination of the elementary excitations and the calculation of the temperature-dependent magnetization and polarization. While the Heisenberg model with DMI shows a Goldstone mode excitation, the ferroelectric subsystem is characterized by a soft mode, i.e., the energy tends to zero at the ferroelectric phase-transition temperature. The mutual coupling between both subsystems modifies the spectrum because the Goldstone mode as well as the soft mode are influenced by the respective other subsystem. Moreover, the interaction energy becomes temperature dependent. As a consequence of the altered excitation spectra, the macroscopic polarization and magnetization, respectively, are simultaneously changed. A further ingredient of our model is the consideration of different spiral structures favored by the DMI. Because such a noncollinear arrangement of spins has no fixed quantization axis, we use a representation of the underlying spin operators with an arbitrary quantization axis. This representation enables us to consider varies spiral alignments.

II. THE HAMILTONIAN

Our model consists of two subsystems. The magnetic part is described by the Heisenberg model and the Dzyaloshinski-Moriya interaction (DMI), where the DMI is essential to include spiral spin arrangements. As mentioned before, the magnetic system is characterized by spin operators $\mathbf{S}_i$ on a lattice at the magnetic lattice at site i. The ferroelectric behavior is stimulated by charge-ordering processes. A typical model to describe such a situation is given by the Ising model in a transverse field.[23] Here we consider, for simplicity, two different charge-ordering positions, which will be characterized by a pseudospin operator P_l^z at the site l of the ferroelectric lattice. The conventional spin operators as well as the pseudospin offer the two eigenvalues $\pm 1/2$. Since we are interested in multiferroics of type I, the coupling between the ferroelectric and the magnetic subsystem is assumed to be weak. Due to Ref. 22, these type-I multiferroics allow a biquadratic coupling in spin $\mathbf{S}$ and the z component of pseudospin operator P^z. The Hamiltonian reads

$$H = H_m + H_p + H_c. \tag{1}$$

The three parts characterize the magnetic subsystem H_m, the ferroelectric (polar) subsystem H_p, and the symmetry-allowed coupling H_c. They are defined by

$$H_m = -\frac{1}{2}\sum_{ij} J_{ij}\mathbf{S}_i\mathbf{S}_j - \frac{1}{2}\sum_{ij}\mathbf{D}_{ij}(\mathbf{S}_i \times \mathbf{S}_j), \tag{2}$$

$$H_p = -\frac{1}{2}\sum_{kl} I_{kl} P_k^z P_l^z - 2\Omega\sum_k P_k^x, \tag{3}$$

$$H_c = -\frac{1}{2}\sum_{ijkl} g_{ijkl}\mathbf{S}_i\mathbf{S}_j P_k^z P_l^z. \tag{4}$$

Here, the magnetic system is characterized by the symmetric isotropic exchange coupling J_{ij} and the relativistic DMI with the antisymmetric coupling vector $\mathbf{D}_{ij}$ between nearest neighbors. The ferroelectric system is identified by the coupling I_{kl} between adjacent double-well potentials situated at lattice points k and l, respectively. The parameter Ω represents the tunnel frequency through the barrier (see Ref. 23). The general form of a biquadratic coupling between both subsystems is introduced in Eq. (4), where g_{ijkl} is the coupling constant between pairs of nearest neighbors. Since we investigate multiferroics of type I with well-separated transition temperatures, the mutual influence of fluctuation on the corresponding other subsystem is assumed to be negligible. Hence, the model can be simplified in a dynamical mean-field approach, leading to the effective coupling strengths

$$\begin{aligned} J_{ij} \to \tilde{J}_{ij} &= J_{ij} + \sum_{kl} g_{ijkl}\langle P_k^z P_l^z\rangle, \\ I_{kl} \to \tilde{I}_{kl} &= I_{kl} + \sum_{ij} g_{ijkl}\langle \mathbf{S}_i\mathbf{S}_j\rangle. \end{aligned} \tag{5}$$

The effective coupling constants become temperature dependent by the averaged values of the other subsystem. Notice that the approximation made in Eqs. (5) can also be reached by a corresponding decoupling of the Green's function, introduced in the subsequent section.

For the description of magnetic systems allowing spiral structure, some special cases have been discussed in earlier papers.[27,28] More recently, noncollinear arrangements have been discussed on a mesoscopic level[12] or within microscopic models.[10,11] In the present paper, we apply a completely different approach by transforming the spin operators into the eigen representation of the quantization axis.[29] Due to the occurrence of spiral structures, the quantization axis is not fixed in a certain direction, but changes by an angle $\varphi_f = \mathbf{Q}\cdot\mathbf{r}_f$ between adjacent spins. This variation is characterized by a spiral wave vector $\mathbf{Q}$, which is determined in the next section. Locally, the direction of the quantization axis is characterized by the real unit vector $\boldsymbol{\gamma}_f = (\gamma_f^x, \gamma_f^y, \gamma_f^z)$. The respective transformation of the spin-$\frac{1}{2}$ operators with $\sigma_f^m = \frac{1}{2} - b_f^+ b_f$ is defined in terms of Pauli operators b^+ and b where, according to Ref. 29, the most general form reads

$$S_f^\alpha = \gamma_f^\alpha \sigma_f^m + A_f^\alpha b_f + (A_f^*)^\alpha b_f^+. \tag{6}$$

The coefficients in Eq. (6) are chosen in such a manner that the commutation relations of spin operators are guaranteed. Using

the realization[29]

$$\begin{aligned}\boldsymbol{\gamma}_f &= \left(\rho_f \cos\varphi_f, \rho_f \sin\varphi_f, \gamma_f^z\right),\\ A_f^x &= -\tfrac{1}{2}\left[\gamma_f^z \cos\varphi_f + \mathrm{i}\sin\varphi_f\right],\\ A_f^y &= -\tfrac{1}{2}\left[\gamma_f^z \sin\varphi_f - \mathrm{i}\cos\varphi_f\right],\\ A_f^z &= \frac{\rho_f}{2} = \frac{1}{2}\sqrt{1-\left(\gamma_f^z\right)^2}, \quad \varphi_f = \mathbf{Q}\cdot\mathbf{r}_f,\end{aligned} \tag{7}$$

the Hamiltonian is transformed into the following compressed form, where only even terms in the annihilation and creation operators has to be taken into account. The magnetic part reads

$$H_m = -\frac{1}{2}\sum_{ij}\left\{X_{ij}^m \sigma_i\sigma_j + 2S_{ij}^m b_i b_j^+ + R_{ij}^m b_i b_j + \tilde{R}_{ij}^m b_i^+ b_j^+\right\}. \tag{8}$$

Using the same procedure, the ferroelectric part is expressed in terms of Pauli operators a and a^+ by

$$\begin{aligned}H_p = &-\frac{1}{2}\sum_{ij}\left\{X_{ij}^p \sigma_i^p \sigma_j^p + 2S_{ij}^p a_i a_j^+ + R_{ij}^p a_i a_j + \tilde{R}_{ij}^p a_i^+ a_j^+\right\}\\ &- 2\Omega\sum_i\left\{\tilde{\gamma}_i^x \sigma_i^p\right\},\end{aligned} \tag{9}$$

with the x component of the unit vector for the ferroelectric subsystem $\tilde{\boldsymbol{\gamma}} = (\sin\vartheta, 0, \cos\vartheta)$. The Fourier-transformed coefficients in front of the Pauli operators are defined in the subsequent section, where the Hamiltonian $H = H_p + H_m$ is studied with the renormalized couplings strengths, according to Eq. (5), by thermodynamic Green's functions.

III. GREEN's FUNCTION

The Green's function method is a powerful tool to elucidate the excitation spectrum of an interacting system, such as the dispersion relation of the elementary excitations of the coupled model (compare Refs. 29 and 30). The spectrum again determines the thermodynamic behavior of the system, in particular, the polarization and the magnetization. The Green's function approach leads to a hierarchy of equations, which will be decoupled in random-phase approximation (RPA). Let us first consider the magnetic subsystem characterized by the Hamiltonian defined in Eq. (8). The corresponding Green's functions are grouped as a 2×2 matrix that obeys, after Fourier transformation, the following equation:

$$\begin{aligned}&\begin{pmatrix}\omega - \varepsilon_1^m(\mathbf{q},\mathbf{Q}) & \varepsilon_2^m(\mathbf{q},\mathbf{Q})\\ -\varepsilon_2^m(\mathbf{q},\mathbf{Q}) & \omega + \varepsilon_1^m(\mathbf{q},\mathbf{Q})\end{pmatrix}\begin{pmatrix}\langle\langle b;b^+\rangle\rangle_{\mathbf{q}} & \langle\langle b;b\rangle\rangle_{\mathbf{q}}\\ \langle\langle b^+;b^+\rangle\rangle_{\mathbf{q}} & \langle\langle b^+;b\rangle\rangle_{\mathbf{q}}\end{pmatrix}\\ &= \begin{pmatrix}2\langle\sigma^m\rangle & 0\\ 0 & -2\langle\sigma^m\rangle\end{pmatrix}.\end{aligned} \tag{10}$$

Here we have introduced the Green's function, using the abbreviation $\langle\langle b(t);b^+(t')\rangle\rangle = -i\Theta(t-t')\langle[b(t),b^+(t')]\rangle$, with $\hbar = 1$. The temperature dependence enters through the thermodynamic mean value within the canonical ensemble. The energy factors in Eq. (10) are given by

$$\begin{aligned}\varepsilon_1^m(\mathbf{q},\mathbf{Q}) &= \langle\sigma^m\rangle[X(0,\mathbf{Q}) - 2S(\mathbf{q},\mathbf{Q})],\\ \varepsilon_2^m(\mathbf{q},\mathbf{Q}) &= 2\langle\sigma^m\rangle R(\mathbf{q},\mathbf{Q}) = \langle\sigma^m\rangle\tfrac{1}{2}\left[\tilde{J}(\mathbf{q}) - \tfrac{1}{2}P(\mathbf{q},\mathbf{Q})\right],\end{aligned} \tag{11}$$

with $X(\mathbf{q},\mathbf{Q}) = -\frac{1}{2}P(\mathbf{q},\mathbf{Q})$, $S(\mathbf{q},\mathbf{Q}) = \frac{1}{4}\tilde{J}(\mathbf{q}) - \frac{1}{8}P(\mathbf{q},\mathbf{Q})$, and $P(\mathbf{q},\mathbf{Q}) = \tilde{J}(\mathbf{q}+\mathbf{Q}) + \tilde{J}(\mathbf{q}-\mathbf{Q}) + \mathrm{i}[D^z(\mathbf{q}-\mathbf{Q}) - D^z(\mathbf{q}+\mathbf{Q})]$. In the last equation, the vector $\mathbf{D}$ of the DMI is assumed to point in the z direction. The spin-waves vector $\mathbf{q}$ and the direction of the propagation of the incommensurate spin spiral with wave vector $\mathbf{Q}$ are determined by the quantization axis $\boldsymbol{\gamma}$. Here we discuss the occurrence of a cycloidal or a screw state, which is related to $\gamma^z = 0$, and so the spiral varies around the z direction. Notice that deviations from the collinear state are characterized by $\gamma^z < 1$, whereas for the parallel aligned state, $\gamma^z = 1$. The wave vector of the spiral $\mathbf{Q}$ is determined by the minimal ground-state energy. It results in

$$\tan(\mathbf{aQ}) = -\frac{D^z}{\tilde{J}}. \tag{12}$$

Here D^z and J are the coupling strengths of the DMI and the isotropic exchange interaction. The poles of the Green's function defined in Eq. (10) yield the dispersion relation of the low-lying states. Directly from Eq. (10) we get, for the magnetic subsystem,

$$\begin{aligned}&\varepsilon^m(\mathbf{q},\mathbf{Q})\\ &= \pm\sqrt{\tfrac{1}{2}\langle\sigma^m\rangle^2\left[\tfrac{1}{2}P(0,\mathbf{Q}) - \tilde{J}(\mathbf{q})\right][P(0,\mathbf{Q}) - P(\mathbf{q},\mathbf{Q})]}.\end{aligned} \tag{13}$$

The dispersion relation of the magnetic system obtained in Eq. (13) is symmetric with respect to the wave vector $\mathbf{q}$ because the renormalized interaction fulfills the condition $P(\mathbf{q},\mathbf{Q}) = P(-\mathbf{q},\mathbf{Q})$. The positive branch of the spin-wave dispersion relation is chosen because a negative excitation energy indicates an instability of the system. In the case of $\gamma^z \neq 0$, the dispersion relation becomes asymmetric, as is demonstrated for pure magnetic systems in Ref. 31. One of the fundamental concepts in different fields is the chirality.[32] In our context, the rotational sense of the spin spiral (chirality) is defined by the interplay between the different interactions within the magnetic subsystem, resulting in the wave vector $\mathbf{Q}$, which is related to a constant canting of spins between adjacent lattice sites. The rotational sense depends on the sign of the DMI, allowing only one type of chirality, which is in accordance with Ref. 33. Here both the symmetric $\tilde{J}_{ij}$ and the antisymmetric interaction D_{ij}^z contribute to the chirality-dependent asymmetry.

The corresponding ferroelectric subsystem is characterized by Eq. (9). In analogy to the magnetic system, let us also introduce Pauli operators for the ferroelectric subsystem (denoted as a and a^+). By using the same procedure,

the 2×2 matrix Green's function satisfies the following equation:

$$\begin{pmatrix} \omega - \varepsilon_1^p(\mathbf{q}) & \varepsilon_2^p(\mathbf{q}) \\ -\varepsilon_2^p(\mathbf{q}) & \omega + \varepsilon_1^p(\mathbf{q}) \end{pmatrix} \begin{pmatrix} \langle\langle a; a^+\rangle\rangle_q & \langle\langle a; a\rangle\rangle_q \\ \langle\langle a^+; a^+\rangle\rangle_q & \langle\langle a^+; a\rangle\rangle_q \end{pmatrix} = \begin{pmatrix} 2\langle\sigma^p\rangle & 0 \\ 0 & -2\langle\sigma^p\rangle \end{pmatrix} \tag{14}$$

with

$$\begin{aligned} \varepsilon_1^p(\mathbf{q}) &= 2\langle\sigma^p\rangle[X^p(0) - 2S^p(\mathbf{q})] + 2\Omega\tilde{\gamma}^x, \\ \varepsilon_2^p(\mathbf{q}) &= 2\langle\sigma^p\rangle R^p(\mathbf{q}). \end{aligned} \tag{15}$$

Here we used $R^p(\mathbf{q}) = \tilde{R}^p(-\mathbf{q}) = \tilde{R}^p(\mathbf{q})$, with

$$X^p(0) = \tilde{I}(0)\cos^2\vartheta, \quad S^p(\mathbf{q}) = \tfrac{1}{2}\tilde{I}(\mathbf{q})\sin^2\vartheta\,. \tag{16}$$

The ferroelectric branch of the dispersion relation reads

$$\varepsilon^p(\mathbf{q}) = \pm\sqrt{[\langle\sigma^p\rangle\tilde{I}(0)\cos^2\vartheta + 2\Omega\tilde{\gamma}^x][\langle\sigma^p\rangle\tilde{I}(0)\cos^2\vartheta + 2\Omega\tilde{\gamma}^x - \langle\sigma^p\rangle\tilde{I}(\mathbf{q})\sin^2\vartheta]} \tag{17}$$

The rotation angle ϑ in the ferroelectric system is determined by the minimal ground-state energy as

$$\sin\vartheta = \frac{2\Omega}{\tilde{I}(0)\langle\sigma^p\rangle}. \tag{18}$$

Thus, Eqs. (13) and (17) determine the excitation spectrum of the coupled multiferroic system. Based on this spectrum, the Green's function technique[29,30] allows the calculation of the averaged polarization according to

$$\langle\sigma^p\rangle = \frac{1}{2}\left\{\sum_{\mathbf{q}} \frac{\varepsilon_1^p(\mathbf{q})}{\varepsilon^p(\mathbf{q})} \coth\left[\frac{\beta}{2}\varepsilon^p(\mathbf{q})\right]\right\}^{-1}. \tag{19}$$

Here β is the inverse temperature in units of the Boltzmann constant. A similar expression is derived for the averaged magnetization $\langle\sigma^m\rangle$, where the ferroelectric dispersion relation $\varepsilon^p(\mathbf{q})$ has to be replaced by the corresponding magnetic one $\varepsilon^m(\mathbf{q})$, according to Eq. (13). Notice that due to Eq. (5), the effective coupling terms can be expressed by the following relations:

$$\begin{aligned} \tilde{J}(\mathbf{q}) &= J(\mathbf{q}) + g(0)\cos^2\vartheta\,\langle\sigma^p\rangle^2\frac{J(\mathbf{q})}{J(0)}, \\ \tilde{I}(\mathbf{q}) &= I(\mathbf{q}) + g(\mathbf{Q})\langle\sigma^m\rangle^2\frac{I(\mathbf{q})}{I(0)}. \end{aligned} \tag{20}$$

Here, the Fourier-transformed ME coupling depends only on the spiral wave vector $\mathbf{Q}$. One observes that the effective magnetic coupling $\tilde{J}(\mathbf{q})$ is influenced by the polarization $\langle\sigma^p\rangle$ and, vice versa, the effective ferroelectric coupling $\tilde{I}(\mathbf{q})$ can be triggered by the magnetization $\langle\sigma^m\rangle$. The analytical results for the magnetization and the polarization are coupled equations, which will be discussed in the subsequent section for the case of the screw state with $\gamma^z = 0$.

IV. DISCUSSION

Using the relation for the magnetization and polarization in the form given by Eq. (19), with $J = 100$ K, $I = 100$ K, transverse field $\Omega = 10$ K, and $D^z = 1$ K, the temperature dependence of the polarization is shown in Fig. 1 for different strengths of the magnetoelectric coupling g. Notice that both the exchange coupling J_{ij} and the DMI D_{ij}^z for the magnetic subsystem, as well as the corresponding coupling I_{ij} for the ferroelectric system, are assumed to be nearest-neighbor couplings. The interaction between both subsystems g_{ijkl}, defined also in Eqs. (4), means a pairwise coupling between the spins and the pseudospins. Due to the set of parameters, the investigated system is ferroelectric up to the ferroelectric phase-transition temperature $T_c = 145$ K, and magnetic up to magnetic transition temperature $T_N = 100$ K. The polarization decreases with increasing temperature and vanishes continuously at the ferroelectric phase-transition temperature T_c. In the region below the magnetic transition temperature T_N, where both the magnetic and the ferroelectric

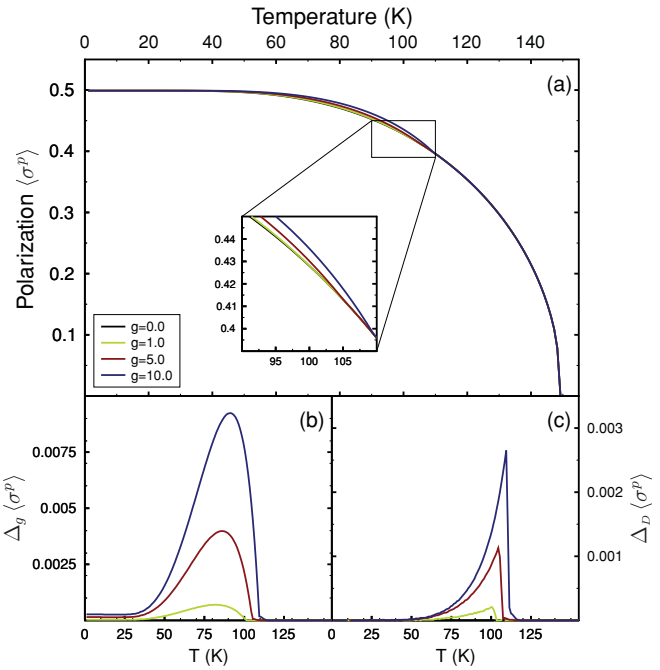

FIG. 1. (Color online) Temperature dependence of the polarization for different strengths of the magnetoelectric coupling for fixed $D^z = 1$ K. (b) Increase of the polarization for different strengths of the ME coupling, $\Delta_g\langle\sigma^p\rangle = \langle\sigma^p\rangle(g) - \langle\sigma^p\rangle(g = 0)$, for fixed $D^z = 1$ K. (c) Additional effect on the polarization for increased DMI, $\Delta_D\langle\sigma^p\rangle = \langle\sigma^p\rangle(D^z = 10\text{ K}) - \langle\sigma^p\rangle(D^z = 1\text{ K})$, for various values of g.

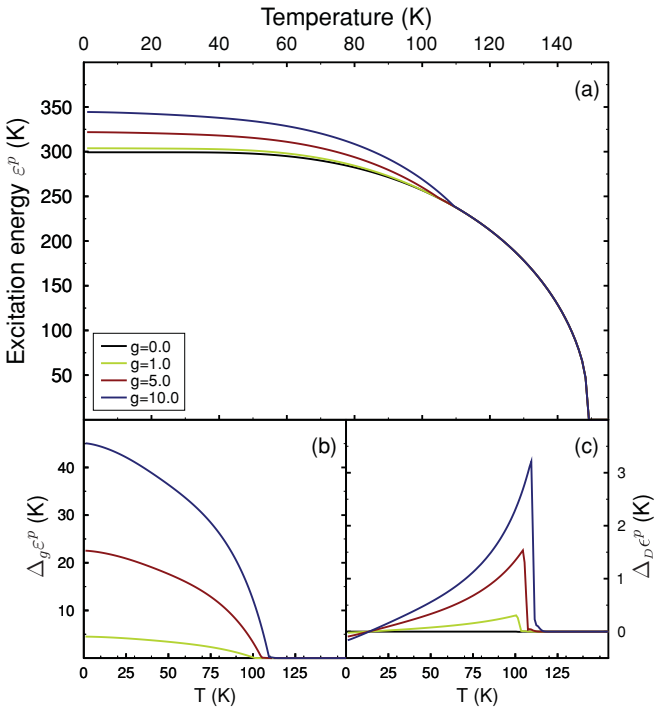

FIG. 2. (Color online) Temperature dependence of the ferroelectric excitation energy ε^p for $\mathbf{q} = 0$ and for different strengths of magnetoelectric coupling g. (b) Change of the excitation energy compared to the noncoupled case, $\Delta_g\varepsilon^p = \varepsilon^p(g) - \varepsilon^p(g = 0)$. (c) Additional effect on the energy for two different strengths of DMI D^z, $\Delta_D\varepsilon^p = \varepsilon^p(D^z = 10\text{ K}) - \varepsilon^p(D^z = 1\text{ K})$. In (a) and (b), the DMI strength is constant at $D^z = 1$ K.

phase may coexist, the polarization is enhanced due to the ME coupling. As expected, a larger ME coupling strength g leads to an enhanced polarization with a more pronounced peak around the magnetic phase transition. The inset shows the magnification of the temperature dependence nearby to the magnetic transition. The enhancement of the polarization due to the ME coupling can be quantified by $\Delta_g\langle\sigma^p\rangle \equiv \langle\sigma^p\rangle(g) - \langle\sigma^p\rangle(g = 0)$ for fixed $D^z = 1$ K. The largest contribution is observed in the vicinity of the magnetic transition. This result is also in accordance with other theoretical findings.[34] In the same manner, one can characterize the influence of the DMI on the polarization defining $\Delta_D\langle\sigma^p\rangle = \langle\sigma^p\rangle(D^z = 10\text{ K}) - \langle\sigma^p\rangle(D^z = 1\text{ K})$. The result is shown in Fig. 1(c). Whereas the ME coupling leads to an enhanced polarization in the whole multiferroic phase, the effect of the spiral structure, driven by the DMI, is considerable only near the magnetic transition. Otherwise it is remarkable that the weak DMI offers an influence of the polarization at all. The ferroelectric excitation energy is likewise influenced in a significant manner by the ME coupling and the DMI, as depicted in Fig. 2. Here, the dispersion relation for $\mathbf{q} = 0$ is shown for different ME coupling strengths at a fixed D^z. The excitation energy offers a soft-mode behavior at the ferroelectric phase transition, i.e., the energy tends to zero in approaching the ferroelectric transition. In the multiferroic phase, where both phases coexist, the excitation energy is enhanced where the most significant contribution occurs for the largest ME coupling strength. The magnetic transition is manifested by the appearance of a kink in the ferroelectric mode. This is in accordance with experiments in the type-I multiferroic $BiFeO_3$. The temperature-dependent Raman spectra of $BiFeO_3$ reveal pronounced phonon anomalies around the magnetic transition temperature.[35] Although we model the ferroelectric subsystem by an order-disorder-like behavior, we believe that the experimental observations made in Ref. 35 reflect some general features of the ME coupling. Our result is also in accordance with a comparable theoretical approach[26] where, however, no spiral magnetic structures are taken into account. For $T > T_N$, where the material is both paramagnetic and ferroelectric, one observes no influence of the magnetic subsystem as expected. Fig. 2(b) shows that the lower the temperature, the more pronounced is the influence of the ME coupling. The weak DMI leads also to an enhancement of the excitation spectrum, as shown in Fig. 2(c). The influence of the DMI on the ferroelectric branch of the excitation energy is presented in more detail in Fig. 3 for a fixed ME coupling, before the ferroelectric mode becomes soft at the ferroelectric transition as already discussed. The magnetic transition is manifested in this ferroelectric soft mode by a kink, which is slightly influenced by the DMI, as shown in the inset of Fig. 3(a). An increasing DMI leads to a magnification of the energy [compare also Fig. 3(b)]. In contrast, the influence of the DMI is not very pronounced at very low temperatures. However, as one can see in Fig. 3(c), the reduced excitation energy at low temperatures is slightly magnified. This effect can be understood by a weakening of the ME coupling strength depending on the vector $\mathbf{Q}$. Notice that this special vector $\mathbf{Q}$, characterizing the spiral structure, is determined implicitly by the ME coupling strength g. The maximum of the effective

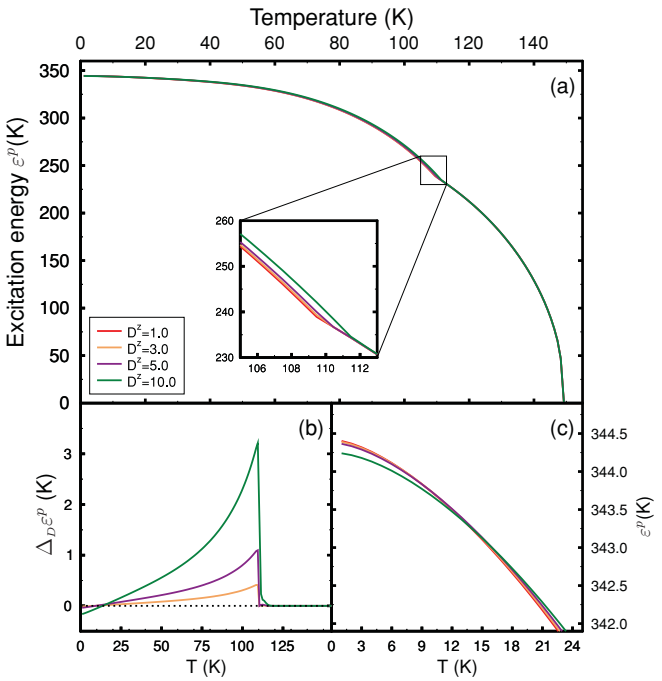

FIG. 3. (Color online) Temperature dependence of the ferroelectric mode ε^p for different strengths of DMI. The inset shows the change in the excitation energy around the magnetic phase transition. (b) Change in energy with increasing strength of DMI, $\Delta_D\varepsilon^p = \varepsilon^p(D^z) - \varepsilon^p(D^z = 1\text{ K})$. (c) Low-temperature behavior of the energy. The ME coupling is $g = 10$ K.

ME coupling strength $g(\mathbf{Q})$ is obviously reached for $\mathbf{Q} = 0$. Hence, a nonzero pitch is related to a reduction of the ME coupling strength g. Furthermore, an enhanced DMI results in a larger pitch $\mathbf{Q}$ of the spin spiral. Otherwise, this additional ordering of the magnetic spins stabilizes the magnetic ordering against temperature fluctuations. The largest enhancement of the ferroelectric excitation energy by the DMI is observed in the vicinity of the magnetic transition, which will be discussed later (compare also Fig. 6). From this and the results presented, we conclude that with increasing temperature, the stabilization of the magnetic phase transition is more dominant than the reduction of the ME coupling by a larger pitch of the spiral. Notice that the stabilization of the magnetic phase is manifested by a shift of the transition temperature to higher values. In the same manner, as in the magnetic case, the macroscopic polarization is determined by the spectrum of its elementary excitations [see Eq. (19)]. As a consequence, the polarization offers an equivalent behavior when the DMI is varied.

Now let us discuss the magnetic subsystem in more detail. In Fig. 4 we show the spin-wave spectrum for small wave vectors $\mathbf{q}$ and different DMI and ME coupling strengths. Even under the influence of the DMI, the magnetic energy remains a Goldstone mode as demonstrated in Fig. 4(a). The dispersion relation within the complete Brillouin zone is depicted in the inset. The influence of the DMI is plotted in Fig. 4(b), while Fig. 4(c) shows the change in the energy for an enlarged ME coupling. Here the largest influence is observed for the lowest DMI strength. This implies a reduction of the ME coupling on the spin-wave spectrum in the case of increasing DMI.

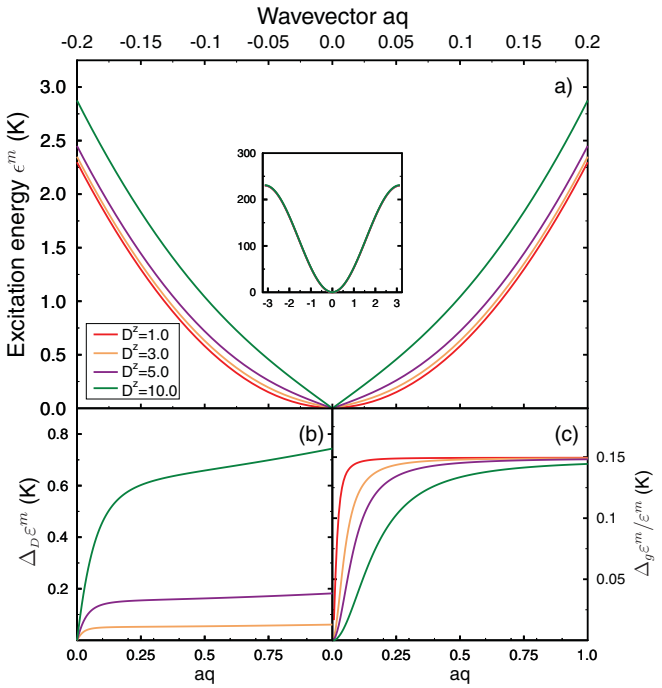

FIG. 4. (Color online) Magnetic dispersion relation ε^m around $\mathbf{q} = 0$ for different strengths of DMI. (b) Deviations in energy for different DMI, $\Delta_D\varepsilon^m = \varepsilon^m(D^z) - \varepsilon^m(D^z = 1\text{ K})$. (c) Change in energy for an enlarged ME coupling, $\Delta_g\varepsilon^m = \varepsilon^m(g = 10\text{ K}) - \varepsilon^m(g = 0)$. In (a) and (b), $g = 10$ K.

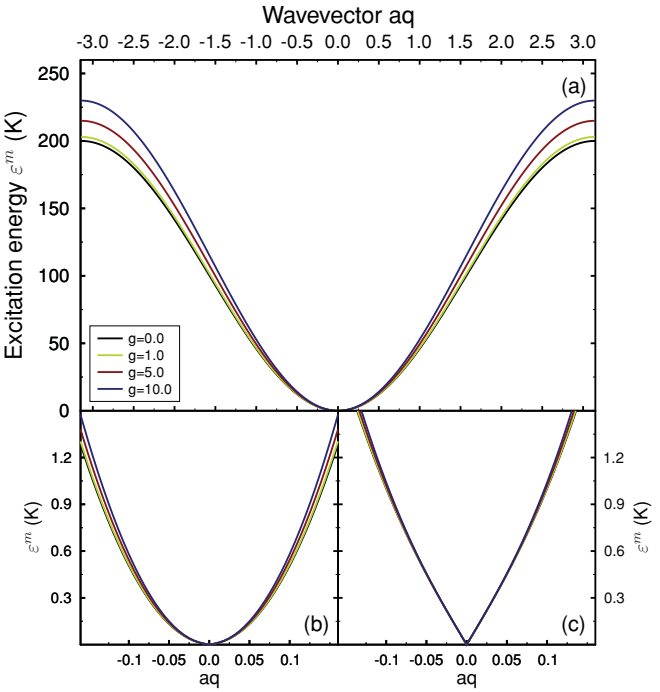

FIG. 5. (Color online) Magnetic dispersion relation ε^m for different strengths of magnetoelectric coupling. (b) Dispersion relation at the Brillouin-zone center. In (a) and (b), the DMI is $D^z = 1$ K, whereas in (c), the dispersion relation for $D^z = 10$ K is plotted.

The influence of the ME coupling is shown in more detail in Fig. 5. With increasing ME coupling, the excitation energy is enhanced mostly at the Brillouin-zone boundary. Obviously, the mutual effect of the DMI and the ME coupling is visible in the spin-wave energy. The excitation energy increases and the curves for different ME coupling become narrower if the DMI is enhanced. This reflects the reduction of the influence of the ME coupling if the DMI enhances. An experimental study of the magnon spectrum in hexagonal multiferroic $YMnO_3$ is carried out in Ref. 36. Here a strong coupling between magnetic and ferroelectric excitations is observed by inelastic neutron scattering in hexagonal multiferroic $YMnO_3$. In our approach, this coupling is manifested in the magnetization presented in Fig. 6. Because the quantization axis of the spins is characterized by the real unit vector $\gamma_f = (\gamma_f^x, \gamma_f^y, 0)$ [see Eq. (6)], the magnetization vector is in the x-y plane. As can be seen, this transverse magnetization decreases with increasing temperature and vanishes continuously at the magnetic transition temperature. With increasing ME coupling, the phase-transition temperature is shifted to higher values [see Fig. 6(a)]. The DMI leads likewise to a stabilization of the magnetization, as shown in Figs. 6(b). In Fig. 6(c) and 6(d), the influence of the ME coupling and the DMI, respectively, is presented on the absolute value of the pitch $|\mathbf{Q}|$. The pitch is determined by the interactions [compare, e.g., Eq. (12)], but varies only in a small range, which was reported experimentally in Ref. 37 for $BiFeO_3$. The observed splitting of the magnetic diffraction maxima suggests the occurrence of a magnetic cycloidal spiral. As the magnetic phase transition is approached, the pitch becomes more pronounced. Our result

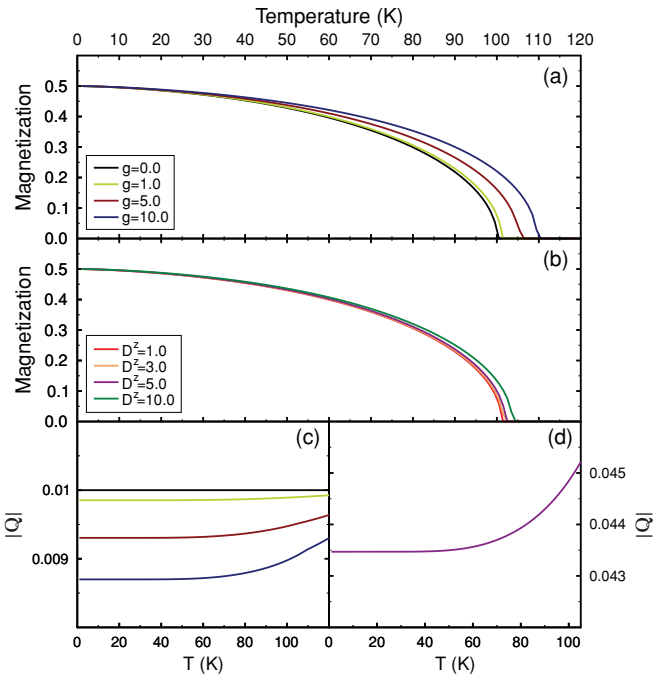

FIG. 6. (Color online) Temperature dependence of the magnetization pointing along the in-plane quantization axis for different (a) ME coupling strengths and (b) DMI strengths. (c) Temperature-dependent pitch for different ME coupling strengths. (d) Pitch $|\mathbf{Q}|$ for the DMI strength $D^z = 5$ K.

reflects the same temperature behavior as observed by the sublattice magnetization measured in $BiFeO_3$.[38]

V. CONCLUSION

The goal of this paper is twofold: to formulate a new microscopic model for the magnetoelectric effect and to find the spectrum of the elementary excitations. We calculate the macroscopic properties of the system, such as the transverse magnetization and the polarization for finite temperatures. As an appropriate tool, the temperature-dependent two-time retarded Green's function is analyzed using the simplest decoupling procedure. The model is comprised of a magnetic, a ferroelectric, and a coupling term. To incorporate the observed spiral structures, the magnetic part of the model is characterized by the Heisenberg model and, additionally, by the Dzyaloshinski-Moriya interaction favoring such spiral states. The ferroelectric behavior is originated from the ordering of dipoles, which allows for simplicity with only two orientations. In that case, the related Hamiltonian is an Ising model in a transverse field. The magnetoelectric coupling between both subsystems is realized by a symmetry-allowed quartic coupling term. In our approach, which reminds us of the dynamical mean-field approximation, the ME coupling leads to a renormalized magnetic exchange interaction by a ferroelectric correlation function. In the same manner, the ferroelectric dipole coupling is modified by a magnetic spin-spin correlation function. As a result, we find the magnetic and the ferroelectric excitation energy as the poles of the corresponding Green's function matrix. Whereas the effective magnetic excitation, modified by the ferroelectric correlation function, remains a Goldstone mode, the effective ferroelectric excitation offers a soft-mode behavior. We conclude that the Goldstone mode and the soft-mode behavior seem to be an inherent property of the applied model. In spite of the ME coupling, such a behavior is retained. As further demonstrated in this paper, the spectrum of the elementary excitations determines the macroscopic quantities as the magnetization and the polarization. Moreover, we have included spiral spin structures in the approach by considering a representation of the underlying spin operators with a varying quantization axis. Although we study type-I multiferroics with well-separated phase-transition temperatures, both the DMI and the ME coupling influence the dispersion relation of the whole system. In particular, the ferroelectric soft mode is changed when the magnetic subsystem undergoes a phase transition, and vice versa. As a consequence, the polarization and the magnetization vary by the occurrence of the coupling due to the mutual influence between both subsystems.

ACKNOWLEDGMENT

T.M. acknowledges support by the International Max Planck Research School for Science and Technology of Nanostructures in Halle.

*thomas.michael@physik.uni-halle.de
†steffen.trimper@physik.uni-halle.de

[1] M. Fiebig, J. Phys. D **38**, R123 (2005).
[2] K. F. Wang, J. M. Liu, and Z. F. Ren, Adv. Phys. **58**, 321 (2009).
[3] J. V. D. Brink and D. I. Khomskii, J. Phys. Condens. Matter **20**, 434217 (2008).
[4] D. Khomskii, Physics (NY) **2**, 1 (2009).
[5] T. Kimura, T. Goto, H. Shintani, K. Ishizaka, T. Arima, and Y. Tokura, Nature (London) **426**, 55 (2003).
[6] T. Goto, T. Kimura, G. Lawes, A. P. Ramirez, and Y. Tokura, Phys. Rev. Lett. **92**, 257201 (2004).
[7] S.-W. Cheong and M. Mostovoy, Nature Mater. **6**, 13 (2007).
[8] M. Kenzelmann, A. B. Harris, S. Jonas, C. Broholm, J. Schefer, S. B. Kim, C. L. Zhang, S.-W. Cheong, O. P. Vajk, and J. W. Lynn, Phys. Rev. Lett. **95**, 087206 (2005).
[9] T. Kimura and Y. Tokura, J. Phys. Condens. Matter **20**, 434204 (2008).
[10] H. Katsura, N. Nagaosa, and A. V. Balatsky, Phys. Rev. Lett. **95**, 057205 (2005).
[11] H. Katsura, A. V. Balatsky, and N. Nagaosa, Phys. Rev. Lett. **98**, 027203 (2007).
[12] M. Mostovoy, Phys. Rev. Lett. **96**, 067601 (2006).

[13]I. E. Dzyaloshinskii, Sov. Phys.-JETP **10**, 628 (1959).
[14]T. Moriya, Phys. Rev. **120**, 91 (1960).
[15]C. D. Hu, Phys. Rev. B **77**, 174418 (2008).
[16]I. A. Sergienko and E. Dagotto, Phys. Rev. B **73**, 094434 (2006).
[17]S. Dong, K. Yamauchi, S. Yunoki, R. Yu, S. Liang, A. Moreo, J. M. Liu, S. Picozzi, and E. Dagotto, Phys. Rev. Lett. **103**, 127201 (2009).
[18]C. Jia and J. Berakdar, Europhys. Lett. **85**, 57004 (2009).
[19]J. P. Perdew, K. Burke, and M. Ernzerhof, Phys. Rev. Lett. **77**, 3865 (1996).
[20]C. Wang, G.-C. Guo, and L. He, Phys. Rev. Lett. **99**, 177202 (2007).
[21]Q. Jiang and S. Gong, Eur. Phys. J. B **43**, 333 (2005).
[22]T. Kimura, S. Kawamoto, I. Yamada, M. Azuma, M. Takano, and Y. Tokura, Phys. Rev. B **67**, 180401 (2003).
[23]R. Blinc and B. Žekš, Adv. Phys. **21**, 693 (1972).
[24]T. Janssen, Ferroelectrics **162**, 265 (1994).
[25]H. Wu, Q. Jiang, and W. Z. Shen, Phys. Rev. B **69**, 014104 (2004).
[26]J. M. Wesselinowa and S. Kovachev, J. Appl. Phys. **102**, 043911 (2007).
[27]T. Kaplan, Phys. Rev. **124**, 329 (1961).
[28]B. Cooper and R. Elliott, Phys. Rev. **131**, 1043 (1963).
[29]S. Tjablikow, *Quantentheoretische Methoden des Magnetismus* (Teubner, Leipzig, 1968).
[30]W. Nolting, *Fundamentals of Many-body Physics* (Springer-Verlag, Berlin, 2009).
[31]T. Michael and S. Trimper, Phys. Rev. B **82**, 052401 (2010).
[32]M. Mochizuki and N. Nagaosa, Phys. Rev. Lett. **105**, 147202 (2010).
[33]M. Bode, M. Heide, K. von Bergmann, P. Ferriani, S. Heinze, G. Bihlmayer, A. Kubetzka, O. Pietzsch, S. Bluegel, and R. Wiesendanger, Nature (London) **447**, 190 (2007).
[34]C. Zhong and J. Fang, Solid State Commun. **128**, 449 (2003).
[35]R. Haumont, J. Kreisel, P. Bouvier, and F. Hippert, Phys. Rev. B **73**, 132101 (2006).
[36]S. Petit, F. Moussa, M. Hennion, S. Pailhes, L. Pinsard-Gaudart, and A. Ivanov, Phys. Rev. Lett. **99**, 266604 (2007).
[37]I. Sosnowska, T. Peterlin-Neumaier, and E. Steichele, J. Phys. C **15**, 4835 (1982).
[38]P. Fischer, M. Polomska, I. Sosnowska, and M. Szymanski, J. Phys. C **13**, 1931 (1980).